

# FLARE ENERGY RELEASE BY FLUX PILE-UP MAGNETIC RECONNECTION IN A TURBULENT CURRENT SHEET

YURI E. LITVINENKO

Institute for the Study of Earth, Oceans, and Space, Morse Hall, University of New Hampshire, Durham, NH 03824-3525; yuri.litvinenko@unh.edu

AND

I. J. D. CRAIG

Department of Mathematics, University of Waikato, Private Bag 3105, Hamilton, New Zealand

Received 2000 May 25; accepted 2000 July 6

## ABSTRACT

The power output of flux pile-up magnetic reconnection is known to be determined by the total hydromagnetic pressure outside the current sheet. The maximum energy-release rate is reached for optimized solutions that balance the maximum dynamic and magnetic pressures. An optimized solution is determined in this paper for a current sheet with anomalous, turbulent electric resistivity. The resulting energy dissipation rate  $W_a$  is a strong function of the maximum, saturated magnetic field  $B_s$ :  $W_a \sim B_s^4$ . Numerically,  $W_a$  can exceed the power output based on the classical resistivity by more than 2 orders of magnitude for three-dimensional pile-up, leading to solar flarelike energy-release rates of the order of  $10^{28}$  ergs  $s^{-1}$ . It is also shown that the optimization prescription has its physical basis in relating the flux pile-up solutions to the Sweet-Parker reconnection model.

*Subject headings:* MHD — Sun: corona — Sun: flares — Sun: magnetic fields

## 1. INTRODUCTION

Although the process of flux pile-up magnetic merging has been known for a long time (Clark 1964; Parker 1973; Sonnerup & Priest 1975; Phan & Sonnerup 1990), recently it became a focus of active research (Inverarity & Priest 1996; Litvinenko, Forbes, & Priest 1996; Watson, Priest, & Craig 1998; Litvinenko & Craig 1999; Craig & Watson 2000a, 2000b). One reason for this is the discovery of exact MHD solutions describing genuine flux pile-up magnetic reconnection, as opposed to simple one-dimensional merging, both in two and in three dimensions (Craig et al. 1995; Craig & Henton 1995; Craig & Fabling 1996). Equally significant is the tantalizing claim that flux pile-up merging allows an increasing rate of magnetic-energy release with reductions in the plasma resistivity. Considering the theoretical difficulty of accounting for rapid energy release in highly conducting astrophysical plasmas, this property alone seems to make the flux pile-up mechanism a prime candidate for explaining solar and stellar flares.

Recent work, however, has emphasized that arbitrary reconnection rates have no physical basis. The main difficulty is that stagnation-point flows, which form the basis of the analytic treatment, eliminate the nonlinear feedback between the magnetic and velocity fields (Craig & Watson 2000a). This decoupling has two unphysical manifestations. The first one is that the amplitude of the stagnation-point flow is independent of the magnetic field strength in the current sheet. Yet even when this problem is addressed—for instance by the optimization process of Litvinenko & Craig (1999), which balances the magnetic and dynamic pressures of the plasma inflow—there remains the specter of unlimited levels of flux pile-up. This problem can be remedied only by assuming a nonlinear saturation condition that essentially imposes an a posteriori bound on the hydromagnetic pressure in the reconnection region (Craig, Fabling, & Watson 1997; Watson & Craig 1997).

The twin notions of optimization and saturation allow plausible bounds to be placed on the reconnection rate of

flux pile-up solutions at realistic coronal resistivities (Litvinenko 1999a; Craig & Watson 2000b). These limits, which apply equally well to two- and three-dimensional reconnection solutions, are remarkably robust; they depend only on the maximum magnetic field in the sheet and the plasma resistivity and remain insensitive to the details of the external region beyond the sheet. It makes no difference, for instance, whether the external pressure is moderated by the dynamic pressure of the inflow (cf. Jardine & Allen 1998) or whether it is regulated by a strong nonreconnecting field component parallel to the sheet (Litvinenko 1999b). A further positive feature is the emergence of the classical Sweet-Parker scaling with resistivity as the saturated limit of the flux pile-up solution. This unification, which seemed puzzling in the classification scheme of Priest & Forbes (1986) for quasi-steady merging solutions, is quite natural when it is realized that the optimization condition results from the plasma exhaust adjusting to the strength of the field in the sheet.

Turning now to the question of magnetic-energy release rates, we note that optimized flux pile-up models allow enhancements of the Sweet-Parker rate typically by factors of 1000. Even so, for plausible levels of flux pile-up, the optimized saturated solutions seem capable of explaining only modest flares, say, with energy-release rates of the order of  $10^{26}$  ergs  $s^{-1}$ , based on classical coronal resistivities  $\eta_c$ . The optimized solutions, however, possess length scales that are very much smaller than the scales in the Sweet-Parker model (Craig & Watson 2000b), and so they are far more susceptible to the breakdown of classical conditions. Specifically, since the predicted sheet thickness is so small, the threshold for a current-driven instability is likely to be exceeded, allowing anomalous resistivity effects to take over. A central goal of this paper is to see how the turbulent electric resistivity affects the energy-release rate of the flux pile-up process.

It is well known from laboratory investigations that the turbulent, anomalous resistivity  $\eta_a$  is proportional to the

applied electric field  $E$ , implying that the electric current density  $j = \text{const}$  (de Kluiver, Perepelkin, & Hirose 1991). This experimental result is consistent with the concept of marginal stability, though specific observational results are hard to interpret theoretically (Bychenkov, Silin, & Uryupin 1988). In the absence of a truly self-consistent treatment, we adopt in this paper an empirical approach in which the properties of turbulent flux pile-up reconnection are derived by taking  $\eta_a \sim E$  as a form of Ohm's law in the turbulent current sheet.

Section 2 of this paper presents the analysis of a particularly simple solution for magnetic merging and gives estimates for the reconnection rate in the turbulent regime. Section 3 shows that the obtained results are not restricted to the simple merging solutions but rather are valid for a wide class of flux pile-up solutions. Moreover, a general argument allows one to establish a close connection between the flux pile-up model and the Sweet-Parker current sheet in both classical and turbulent regimes. Section 4 summarizes our findings.

2. AN ANALYTICAL MODEL FOR FLUX PILE-UP MERGING

2.1. Introduction

It is now understood that the nature of three-dimensional reconnection depends, in large measure, on the eigenstructure of the magnetic null point. The implication is that

magnetic merging can assume one of three forms, typified by spine, fan, and separator reconnection models (Priest & Titov 1996; Lau & Finn 1990; for a review see Priest & Forbes 2000). Of these, only separator merging does not require reconnection to occur at a neutral point; it is sufficient to have a planar null, threaded by an axial field that runs perpendicular to the reconnecting field lines. In such cases reconnection is sustained by a strong ribbon of current aligned to the axial field. If sufficiently strong, the axial field may in turn provide the bulk of the external hydromagnetic pressure required to drive the reconnection.

Figure 1 contrasts the current ribbon of separator merging with the current layer of fan reconnection. Unlike spine reconnection, which involves quasi-cylindrical currents aligned to the spine, both separator and fan mechanisms are associated with the development of current sheets (as represented by shaded planes of negligible thickness in the diagrams). In the fan model distortions of the spine cause a current sheet to accumulate over the fan—the plane defined by field lines emanating from the null. By contrast, in the separator model the plane drawn perpendicular to the current ribbon is not associated with a neutral point. The dashed lines in this plane therefore indicate only projected field lines (Craig & Fabling 1996).

The aim of this paper is to apply the notions of optimization and saturation to planar reconnection sustained by a strong axial field (Litvinenko 1999b). Our approach is

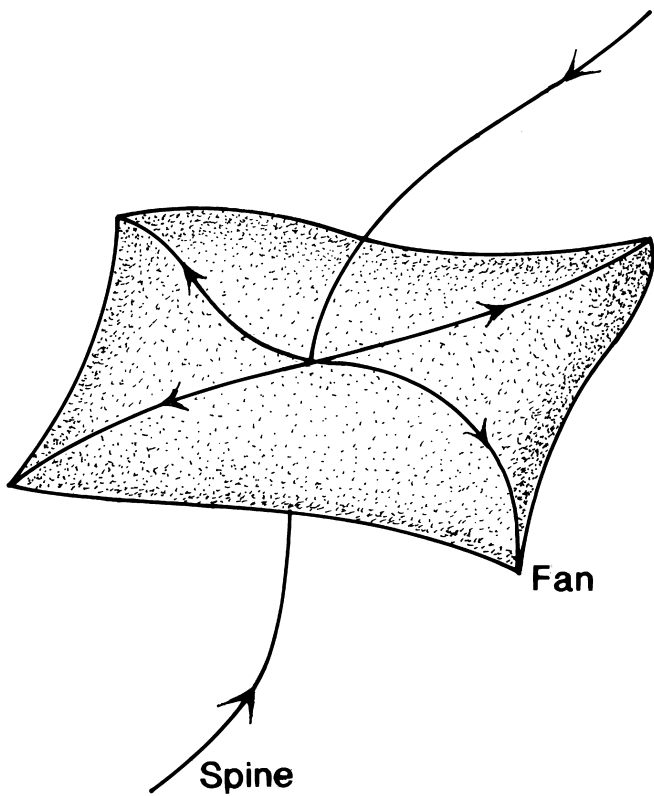


FIG. 1a

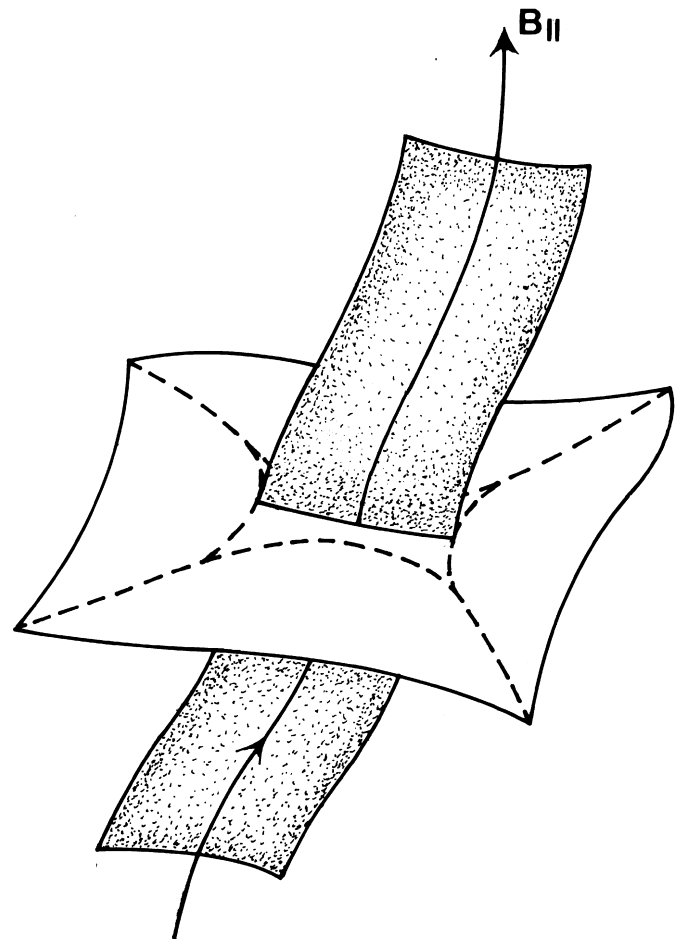


FIG. 1b

FIG. 1.—Illustration of (a) fan and (b) separator reconnection geometries

complementary to that of Craig & Watson (2000b) who consider optimized three-dimensional, analytic spine and fan reconnection solutions. Craig & Watson (2000b) concluded that, although the quasi-cylindrical current structures of spine models seem incapable of substantial flarelike energy-release, optimized fan models involving quasi-one-dimensional current sheets appear more promising. In fact, the ohmic dissipation rates of all fan solutions reduce to the optimized, saturated limit deduced by Litvinenko & Craig (1999) on the basis of a simpler planar analysis. This rate, which is a significant improvement on earlier nonoptimized saturated power outputs for fan solutions (Craig et al. 1997; Watson & Craig 1997), is remarkably insensitive to the conditions external to the sheet; all that really matters is that the external region can provide sufficient hydromagnetic pressure and magnetic flux to sustain the current sheet. Both Litvinenko (1999b) and Craig & Watson (2000b), however, mainly concentrate on collisional resistivities. We show in this paper, on the basis of a concrete merging solution involving a purely planar null, that significant gains are to be expected when turbulent enhancements of the resistivity are considered. The general nature of these scalings is further emphasized in § 3.

### 2.2. The Planar Merging Solution

We begin by writing down the system of incompressible inviscid resistive steady state MHD equations in the standard notation:

$$\rho(\mathbf{v} \cdot \nabla)\mathbf{v} = -\nabla p + \mathbf{j} \times \mathbf{B}/c, \quad (1)$$

$$\mathbf{E} + \mathbf{v} \times \mathbf{B}/c = \eta \mathbf{j}, \quad (2)$$

where  $\nabla \times \mathbf{E} = 0$  and the electric current  $\mathbf{j} = c\nabla \times \mathbf{B}/4\pi$ . As distinct from the previous treatments (Litvinenko 1999a; Litvinenko & Craig 1999), the resistivity is not assumed to have a classical value but rather can be determined by plasma turbulence in the current sheet. Another difference has to do with the geometry of the magnetic field  $\mathbf{B}$ . Since a large axial, nonreconnecting component  $B_a$  of the field is known to mitigate the pressure limitation on the reconnection rate (Litvinenko 1999b), we consider a model (Craig et al. 1995) with both the reconnecting  $B_r$  and the axial  $B_a$  field components:

$$\mathbf{B} = \mathbf{B}_r + \mathbf{B}_a. \quad (3)$$

For simplicity, we assume that the magnetic field depends only on one space coordinate:

$$\mathbf{B} = [B_r(y), 0, B_a(y)]. \quad (4)$$

The only allowable velocity field (Craig & Henton 1995) is the stagnation-point flow solution

$$\mathbf{v} = [xf'(y) - f(y)], \quad (5)$$

where, taking the curl of equation (1),

$$f'f'' = ff'''. \quad (6)$$

Solutions comprise linear, sinusoidal, and hyperbolic inflow models. These velocity fields describe two plasma streams colliding at the plane  $y = 0$ , where a current sheet is located.

As usual, it is convenient to define reference, “external” values of the plasma inflow speed  $v_e$  and the reconnecting magnetic field  $B_{r,e}$  at some boundary  $y = L_e$  that defines a global length scale. A conventional measure of the flux transfer rate is the Alfvén Mach number  $M = v_e/v_{A,e}$ , where

$v_{A,e} = B_{r,e}/(4\pi\rho)^{1/2}$  is the Alfvén speed and  $\rho$  is the mass density.

In what follows we consider flow solutions specified by the inflow vorticity imposed at the external boundary. The profile that has just enough freedom to “optimize” the merging solution is the sinusoidal inflow

$$f = v_e \frac{\sin(\lambda y/L_e)}{\sin \lambda}, \quad (7)$$

where  $0 \leq \lambda < \pi$  is a vorticity parameter (Jardine et al. 1992). Using this profile in equation (2) for steady pile-up with the reconnection electric field  $E_z = E = \text{const}$ , results in equations for the magnetic field components:

$$fB'_a + \frac{\eta c^2}{4\pi} B'_a = 0, \quad (8)$$

$$fB_r + \frac{\eta c^2}{4\pi} B_r = cE. \quad (9)$$

Thus not only the flow dynamics are independent of the magnetic field dynamics, but also the reconnecting and non-reconnecting field components are independent of each other. It is this property that allows one to obtain the exact analytical MHD solutions for flux pile-up reconnection (Craig & Henton 1995; Craig & Fabling 1996). Unfortunately, it also means that the lack of feedback between the plasma flow and the magnetic field makes it impossible to specify unambiguously the reconnection rate from the solution itself.

### 2.3. Optimization and Saturation Conditions

Following Litvinenko & Craig (1999), we argue that the maximum reconnection rate is realized for the “optimized” solution for which both dynamic and magnetic-energy densities do not exceed the total external pressure (cf. Jardine & Allen 1998; Zweibel 1998). As Craig & Watson (2000b) have emphasized, and as we shall demonstrate explicitly for the merging solution at hand, this condition is equivalent to tuning the exhaust flow of material expelled from the sheet to correspond to the Alfvén speed at the entrance to the current sheet. This basic assumption, which underlies the classical Sweet-Parker merging rate, optimizes the solution in that it gives the thinnest sheet with the most favorable energy-release properties.

In the low-beta plasma of the solar corona, the pressure is defined by the axial magnetic-field energy density. The axial field is derived from equation (8) by quadrature. For example, in the case of a linear velocity profile  $f \sim y$ , an error function solution is obtained for  $B_a$ , and the reconnecting component  $B_r$  is described by the Dawson function (Craig et al. 1995). For the velocity profile given by equation (7), the simplest way to model a strong axial field in solar coronal loops is to take

$$B_a = \text{const} \gg B_{r,e}. \quad (10)$$

Then the optimization prescription takes the form

$$\rho v_{\text{max}}^2/2 = B_{r,\text{max}}^2/8\pi = B_a^2/8\pi. \quad (11)$$

Well-defined merging rates can now be deduced by imposing a saturation condition that limits the amplitude of the reconnecting field in the sheet. This corresponds simply to applying a bound on the axial field magnitude  $B_a$  valid for all resistivities  $\eta$ .

#### 2.4. The Anomalous Resistivity

To proceed further it is necessary to define the anomalous electric resistivity. In agreement with the marginal stability argument (Bychenkov et al. 1988) and numerous laboratory investigations (de Kluiver et al. 1991), we assume that the anomalous enhanced resistivity is proportional to the local electric field:

$$\frac{\eta_a}{\eta_c} \approx 10 \frac{E}{E_D} \quad (12)$$

for  $E > E_D$  (LaRosa 1992). Here  $E_D$  is the Dreicer electric field:

$$E_D = \frac{4\pi n e^3 \ln \Lambda}{kT}, \quad (13)$$

where  $n$  and  $T$  are the density and temperature in the sheet and  $\eta_c \sim T^{-3/2}$  is the classical resistivity. Thus our treatment is not completely self-consistent in that we have to rely on plasma physics results in addition to the MHD analysis. We believe this to be a reasonable first step in the study of flux pile-up magnetic reconnection in a turbulent plasma.

An important consequence of equation (12) is that the electric current density is independent of the local electric field:

$$j \approx J = 0.1 \frac{E_D}{\eta_c} \approx \text{const}. \quad (14)$$

It is hard to make a definitive choice for the parameters of a current sheet in the solar corona. Here and in what follows we take as reference coronal parameters the values of  $T = 10^6$  K,  $n = 10^9$  cm<sup>-3</sup>,  $L_e = 10^{9.5}$  cm,  $B_{r,e} = 10^2$  G, and  $B_a = 10^3$  G. These values lead to  $\eta_c \approx 10^{-16}$  s,  $E_D \approx 10^{-7}$  cgs, and  $J \approx 10^8$  cgs. Note that  $8\pi n k T \ll B_{r,e}^2$ , which is consistent with the assumed dominant axial field  $B_a$ .

#### 2.5. The Boundary-Layer Solution

To determine the profile of the reconnecting magnetic field  $B_r$  analytically, we perform a boundary-layer analysis of equation (9) based on the smallness of  $\eta$  outside the current sheet. The dissipation is negligible there, and an asymptotic solution is obtained by setting  $\eta = 0$ :

$$B_{r,\text{out}}(y) \approx B_{r,e} \frac{\sin \lambda}{\sin(\lambda y/L_e)}. \quad (15)$$

Inside the sheet  $\eta = \eta_a$ , and the resistive term dominates, leading to a linear field profile:

$$B_{r,\text{in}}(y) \approx \frac{4\pi}{c} J y. \quad (16)$$

The current sheet (half-) thickness is defined by the location  $y = l$ , where the outer and inner expansions become comparable:

$$l \approx \left( \frac{c B_{r,e} L_e \sin \lambda}{4\pi J \lambda} \right)^{1/2}. \quad (17)$$

The maximum magnetic field is reached at the entrance to the sheet and is found by substituting  $l$  into either equation (15) or (16):

$$\frac{B_{r,\text{max}}}{B_{r,e}} \approx \left( \frac{4\pi J L_e \sin \lambda}{c B_{r,e} \lambda} \right)^{1/2}. \quad (18)$$

Equations (7), (15), (16), and (17) give the complete formal solution of the problem. It remains only to determine the optimized reconnection rate.

We now adopt equation (11) to make sure that the pressures associated with the maximum inflow speed  $v_{\text{max}} = v_e/\sin \lambda$  and the maximum magnetic field in equation (18) do not exceed the external pressure determined by the axial, nonreconnecting field component  $B_a$ . Equation (11) results in two equations for optimized values of  $\lambda$  and  $v_e$ . Straightforward algebra leads to the sought after optimized solution:

$$\sin \lambda \approx \frac{c B_{r,e}}{4J L_e} \left( \frac{B_a}{B_{r,e}} \right)^2, \quad (19)$$

$$M \approx \frac{c B_{r,e}}{4J L_e} \left( \frac{B_a}{B_{r,e}} \right)^3, \quad (20)$$

where the last result is expressed in terms of the Alfvén Mach number. Note that  $\lambda \approx \pi$  and  $\sin \lambda \ll 1$  for the assumed parameters. Numerically, the maximum merging rate is  $M \approx 3 \times 10^{-3}$  for the reference parameters  $B_{r,e} = 10^2$  G,  $B_a = 10^3$  G, and  $L_e = 10^{9.5}$  cm. This is a significant improvement on the results for the classical electric resistivity. In particular, the maximum  $M$  corresponds to the inflow speed  $v_e \approx 30$  km s<sup>-1</sup> and the electric field  $E \approx 3$  V cm<sup>-1</sup>  $\gg E_D$ . These numbers strongly suggest that turbulent reconnection due to flux pile-up can be responsible for large solar flares. It is also worth noting that the flux pile-up mechanism is more efficient in resistive energy dissipation rather than flux transfer away from the reconnection site. This is why strong resistive heating should be a signature of flux pile-up reconnection.

Equations (19) and (20) can be substituted into equation (17) to find the optimized sheet thickness  $l = c B_a / 4\pi J$ , which is a physically obvious result. It is worth pointing out another result that sheds light on the physical nature of the optimization prescription (11). For the optimized  $\sin \lambda$  and  $v_e = M v_{A,e}$  from equations (19) and (20), it follows from equations (5) and (7) that the outflow from the current sheet ( $x = L_e, y = 0$ ) occurs with the speed

$$v_{\text{out}} \approx \frac{\pi B_{r,\text{max}}}{\sqrt{4\pi\rho}}, \quad (21)$$

which is of the order of the local Alfvén speed in the sheet. Thus, as already mentioned, the optimization prescription automatically leads to Alfvén outflows from the reconnection region in the exact flux pile-up solution.

### 3. GENERAL ANALYSIS AND PREDICTED POWER OUTPUT

#### 3.1. Introduction

As the previous analytic model suggests, the formation of thin flux pile-up current sheets can result in the breakdown of classical electric resistivity and a significant increase of the reconnection rate. We now proceed to show that this result is quite general. In fact, it appears that the basic ideas of optimization and saturation, introduced in § 2, are valid for any flux pile-up reconnection solution with a quasi-one-dimensional current sheet, including the fully three-dimensional “fan” reconnection (Craig et al. 1995). Moreover, a general argument suggests that the values of the

energy-release rate and the reconnection electric field are of the order of those required in energetic solar flares.

Recall that a significant drawback of all analytic solutions for flux pile-up reconnection is the assumed form of the stagnation-point inflow profile  $v$ , which eliminates the nonlinear feedback between the magnetic field and the plasma flow. This feedback is effectively restored by the optimization and saturation constraints. The optimization gives

$$B_{r, \max}^2/8\pi = \rho v_{\max}^2/2, \quad (22)$$

while the saturation condition sets an upper limit on the magnetic field  $B_{r, \max}$  at the onset of the current layer:

$$B_{r, \max} \leq B_s. \quad (23)$$

For planar models in a strictly two-dimensional setting, the upper limit on the reconnecting field  $B_s$  is defined by the hydromagnetic pressure at some reference inflow boundary; in a more general setting it may be determined by the strength of the axial, nonreconnecting component. The following argument shows that the optimization and saturation constraints lead to a well-defined limit on the rate of flux pile-up merging (Litvinenko 1999a, 1999b; Litvinenko & Craig 1999; Craig & Watson 2000b), which reduces to the Sweet-Parker scaling when uniform external conditions are assumed beyond the sheet. This relation was not clear in the past (Priest & Forbes 1986).

It should be emphasized that equation (22) only requires the plasma speed not to exceed the maximum Alfvén speed in the reconnection inflow region. It is a nontrivial consequence of the optimization prescription that the reconnection outflow speed, given by equation (21), is also defined by the Alfvén speed based on the maximum magnetic field at the entrance to the sheet.

To obtain concrete numbers, we adopt the reference parameters of § 2; that is, we normalize the reconnecting magnetic field by a typical coronal value  $10^2$  G, the distance by a typical coronal active region scale  $10^{9.5}$  cm, and the plasma bulk speed by the Alfvén speed  $v_A = 10^9$  cm s<sup>-1</sup>, corresponding to the number density of  $10^9$  cm<sup>-3</sup> in flare loops. Note that the dimensionless classical electric resistivity  $\eta_c$  in these units is very small; it is the inverse Lundquist (magnetic Reynolds) number of the order of  $10^{-14.5}$ . To model the coronal magnetic field, we also assume the presence of a strong axial (nonreconnecting) field component  $B_a$  that can exceed  $B_r$  by as much as an order of magnitude (Litvinenko 1999b).

### 3.2. Results for Classical Resistivities

For completeness, we begin by considering the case when the electric resistivity remains classical. The treatment is very similar when the resistivity is turbulent. The power of the argument below is that there is no need to specify the inflow velocity profile. All that matters is that the inflow speed at the stagnation point itself is zero and that the first nonzero term is proportional to distance in all known solutions. Technically, we require only that the inflow velocity remains linear over the thickness of the sheet (Craig & Watson 2000b).

The inflow speed  $v_{\text{in}}$  at the entrance to the current sheet has to be balanced by magnetic diffusion:

$$v_{\text{in}} = \alpha l = \eta_c/l, \quad (24)$$

where  $l$  is the current sheet thickness and  $\alpha$  is a constant. Again, for the stagnation-point flow,  $\alpha$  is simply the outflow speed from the reconnection region  $v_{\text{out}}$ . The optimization assumption requires the outflow to be given by the local Alfvén speed in the sheet. In dimensionless form

$$v_{\text{out}} = \alpha = B_{r, \max}. \quad (25)$$

Finally, the saturation assumption demands that the external hydromagnetic pressure sets an upper limit on the magnetic field at the sheet entrance:

$$B_{r, \max} = B_s. \quad (26)$$

The saturated field  $B_s$  is set here by the axial, nonreconnecting component. For illustrative purposes, we assume that  $B_s = 10$ , corresponding to a kilogauss local field (Litvinenko 1999b).

The last three equations are easily solved to give the current sheet thickness

$$l = (\eta_c/B_s)^{1/2} \quad (27)$$

and the inflow speed to the sheet

$$v_{\text{in}} = (\eta_c B_s)^{1/2}. \quad (28)$$

It is of great importance that the scalings of  $l$  and  $v_{\text{in}}$  with  $\eta_c$  are the same as those for the Sweet-Parker current sheet (Litvinenko & Craig 1999). The flux pile-up model is made locally a particular case of the Sweet-Parker reconnection model by using the optimization assumption to specify the outflow speed.

Note that the local equivalence of the two models does not make them identical globally. The argument above is different from the usual analysis for the Sweet-Parker current sheet. The Sweet-Parker solution is almost uniform,  $B_s \approx 1$ , in the inflow region (Priest & Forbes 1986), whereas  $B_s \gg 1$  is possible for the nonuniform inflow conditions of pile-up models (Craig & Watson 2000a, 2000b). For the particular model of § 2, equation (15) confirms that the field falls off rapidly in the outer region and does not depend on the assumed resistivity in the current layer. It is the strong flux pile-up that is ultimately responsible for superior power output in the flux pile-up model as compared with the Sweet-Parker current sheet.

To estimate the energy-release rate by flux pile-up reconnection, consider the rate of ohmic dissipation per unit area of the current sheet:

$$W_c = \eta_c B_s^2/l = \eta_c^{1/2} B_s^{5/2} \approx 2 \times 10^{-5}. \quad (29)$$

This result, first obtained by Litvinenko & Craig (1999) for planar merging, has recently been shown to apply to all three-dimensional fan-current reconnection solutions (Craig & Watson 2000b). The result also follows by evaluating the saturated Poynting flux  $v_{\text{in}} B_s^2$  into the sheet. For the inverse Lundquist number  $\eta_c = 10^{-14.5}$ ,  $W_s \approx 6 \times 10^{25}$  ergs s<sup>-1</sup> in dimensional units can only explain a very small solar flare.

The thickness of the current layer in the present model is only  $l \approx 50$  cm. This is almost 5 orders of magnitude less than the collisional mean free path

$$l_{\text{mfp}} = \frac{9(kT)^2}{16\pi n e^4 \ln \Lambda} \approx 3 \times 10^6 \text{ cm} \quad (30)$$

for  $T = 10^6$  K and  $n = 10^9$  cm $^{-3}$  (e.g., Sivukhin 1966). The smallness of  $l$  inevitably leads to large electric current densities and the breakdown of collisional conditions in sheet. Therefore it is necessary to consider the anomalous, turbulent resistivity in the sheet.

### 3.3. Results For Turbulent Resistivities

It is easy to modify the argument above to account for turbulent resistivity. Equations (25) and (26) remain valid, and we only have to replace equation (24) by the appropriate form of Ohm's law:

$$B_{r, \max}/l = J = \text{const}, \quad (31)$$

where  $J = 10^6$  in our dimensionless units (eq. [14]). This modification leads to scalings for the current sheet thickness

$$l = B_s/J \quad (32)$$

and the inflow speed

$$v_{\text{in}} = B_s^2/J. \quad (33)$$

Note for clarity that  $v_{\text{in}}$  is the inflow speed at the entrance to the sheet (a distance  $l \ll 1$  from the neutral plane). Hence its scaling is different from that for the inflow speed at the boundary  $v_e = B_s^3/J$ , which is given by equations (20) and (35) below.

The rate of ohmic dissipation per unit area of the turbulent current sheet  $W_a$  is determined to be a strong function of the pile-up factor  $B_s$ :

$$W_a = v_{\text{in}} B_s^2 = B_s^4/J \approx 10^{-2}, \quad (34)$$

which translates into  $10^{28}$  ergs s $^{-1}$  in dimensional units. The power output increases significantly in the turbulent regime:  $W_a/W_c \approx 5 \times 10^2$ . Although this result can be interpreted as an effective increase of electric resistivity by a factor of  $10^4$ – $10^5$  (cf. eq. [29]), this interpretation can be misleading given that the improvement factor is a function of the assumed coronal parameters.

Two other points are worth making. First, the reconnection electric field associated with flux pile-up reconnection,

$$E = v_{\text{in}} B_s = B_s^3/J, \quad (35)$$

is indeed highly super-Dreicer. The dimensionless estimates above correspond to fields of the order of  $10^{-2}$  cgs  $\approx 3$  V cm $^{-1}$ . The same result for the particular model of § 2 follows from equation (20) since  $E = Mv_{A, e} B_e/c$ . This estimate has important implications for particle acceleration at sites of magnetic reconnection. Efficient particle acceleration by the DC electric field should be a signature of rapid reconnection, and electric fields of the order of a few V cm $^{-1}$  appear to be necessary to explain, for example, the observed hard X-ray emission in solar flares (e.g., Litvinenko 1996). Note also that the total electric current  $I$  through the sheet in the optimized saturated solution is in nice agreement with observations of nonpotential magnetic fields in solar active regions:

$$I = 2JL_e = \frac{1}{2\pi} cL_e B_a \approx 6 \times 10^{12} \text{ A}. \quad (36)$$

The second point of interest is that the thickness of the current sheet  $l$  in the turbulent regime becomes much larger,

as one would expect on physical grounds. Equation (32) leads to  $l \approx 10^{-5}$ , implying that  $l \approx 3 \times 10^4$  cm. The sheet thickens by almost a factor of  $10^3$  in the turbulent regime. It may be of interest that the characteristic length scale of turbulent reconnection is a significant fraction of the collisional mean free path  $l_{\text{mf,p}} \approx 3 \times 10^6$  cm. It follows from equations (14), (30), and (32) that  $l/l_{\text{mf,p}} \sim T^{-5/2}$  is independent of density, making the result more robust with respect to the assumed parameters. Strong heating, however, may eventually lead to a purely collisionless reconnection regime. In any case, the relatively large value of  $l$  in the turbulent current sheet mitigates the shortcoming of the flux pile-up solutions based on classical resistivity, which predicted the current sheet thickness to be less than  $10^2$  cm. Such a small length scale would inevitably lead to very large current densities exceeding the threshold for a current-driven instability. Including the anomalous resistivity in the sheet into consideration makes the pile-up solution more self-consistent.

## 4. DISCUSSION

Our main motivation in this paper is to explore whether flux pile-up magnetic reconnection can provide rapid, flare-like release of magnetic energy. Although the rate of energy release is severely limited by the total external hydro-magnetic pressure in the corona (Litvinenko & Craig 1999), we have identified two ways to mitigate the limitation. First, the external pressure itself increases in three-dimensional geometries with a strong axial magnetic field (Litvinenko 1999b; Craig & Watson 2000b). Second, as demonstrated in this paper, the power output can be increased by more than 2 orders of magnitude by taking into account the turbulent electric resistivity in the current sheet. The central result is given by equation (34). The energy-release rate by flux pile-up reconnection at a single reconnection site in the corona can reach  $10^{28}$  ergs s $^{-1}$ , which corresponds to quite powerful solar flares. Moreover, the model predicts the electric field of the order of a few V cm $^{-1}$  at the reconnection site, which is enough to account for efficient particle acceleration and nonthermal flare emissions.

It should be emphasized that turbulent resistivity alone is not enough to bring about rapid reconnection and energy release in the Sweet-Parker current sheet (LaRosa 1992). It is the advantage of flux pile-up reconnection that the local magnetic field at the entrance to the current sheet is built up significantly, leading to larger electric current densities, thinner sheets, faster exhaust speeds, and enhanced ohmic dissipation.

Another interesting result of the present study is the intimate relation between the pile-up solutions and the Sweet-Parker reconnection model. We established earlier that the maximum rate of flux pile-up reconnection is realized for “optimized” solutions that are characterized by equal dynamic and magnetic pressures (Litvinenko & Craig 1999). The optimization prescription is necessary in the analytical approach since the original pile-up solution decouples the dynamics of the plasma flow and magnetic field, so that arbitrary reconnection rates appear formally possible. The optimization and saturation assumptions remove the ambiguity in a natural way. The analysis shows that the optimized solution is locally equivalent to the Sweet-Parker current sheet—a relation that was far from clear in the past (Priest & Forbes 1986).

Finally, we wish to stress that the analytical results

derived for simple exact solutions (Craig & Henton 1995; Craig & Fabling 1996) have a wide range of applicability. The three-dimensional spine and fan-current analysis of Craig and Watson (2000b) confirm that the ohmic dissipation rate we derive can be applied to any flux pile-up model with a quasi-one-dimensional current sheet. Analysis of these exact solutions should be a powerful tool in the reconnection theory. Possible applications may include analysis of MHD stability of the reconnecting current sheet and the use of the self-consistent electric and magnetic field

structure to study the acceleration of charged particles to suprathermal energies.

One of the authors (Y. E. L.) is grateful to I. J. D. Craig and his colleagues from the Department of Mathematics at the University of Waikato for their generous hospitality. This work was supported by NSF grant ATM 98-13933, NASA grant NAG 5-7792, and a New Zealand Marsden Fund award.

## REFERENCES

- Bychenkov, V. Y., Silin, V. P., & Uryupin, S. A. 1988, *Phys. Rep.*, 164, 119  
 Clark, A. 1964, *Phys. Fluids*, 7, 1299  
 Craig, I. J. D., & Fabling, R. B. 1996, *ApJ*, 462, 969  
 Craig, I. J. D., Fabling, R. B., Henton, S. M., & Rickard, G. J. 1995, *ApJ*, 455, L197  
 Craig, I. J. D., Fabling, R. B., & Watson, P. G. 1997, *ApJ*, 485, 383  
 Craig, I. J. D., & Henton, S. M. 1995, *ApJ*, 450, 280  
 Craig, I. J. D., & Watson, P. G. 2000a, *Sol. Phys.*, 191, 359  
 ———. 2000b, *Sol. Phys.*, 194, 251  
 de Kluiver, H., Perepelkin, N. F., & Hirose, A. 1991, *Phys. Rep.*, 199, 281  
 Inverarity, G. W., & Priest, E. R. 1996, *Phys. Plasmas*, 3, 3591  
 Jardine, M., & Allen, H. R. 1998, *Sol. Phys.*, 177, 411  
 Jardine, M., Allen, H. R., Grundy, R. E., & Priest, E. R. 1992, *J. Geophys. Res.*, 97, 4199  
 LaRosa, T. N. 1992, *ApJ*, 396, 289  
 Lau, Y.-T., & Finn, J. M. 1990, *ApJ*, 350, 672  
 Litvinenko, Y. E. 1996, *ApJ*, 462, 997  
 ———. 1999a, *Sol. Phys.*, 186, 291  
 Litvinenko, Y. E. 1999b, *Sol. Phys.*, 188, 115  
 Litvinenko, Y. E., & Craig, I. J. D. 1999, *Sol. Phys.*, 189, 315  
 Litvinenko, Y. E., Forbes, T. G., & Priest, E. R. 1996, *Sol. Phys.*, 167, 445  
 Parker, E. N. 1973, *J. Plasma Phys.*, 9, 49  
 Phan, T. D., & Sonnerup, B. U. Ö. 1990, *J. Plasma Phys.*, 44, 525  
 Priest, E. R., & Forbes, T. G. 1986, *J. Geophys. Res.*, 91, 5579  
 ———. 2000, *Magnetic Reconnection: MHD Theory and Applications* (Cambridge: Cambridge Univ. Press), chap. 8  
 Priest, E. R., & Titov, V. S. 1996, *Philos. Trans. R. Soc. London, A*, 354, 2951  
 Sivukhin, D. V. 1966, in *Reviews of Plasma Physics* 4, ed. M. A. Leontovich (New York: Consultants Bureau), 93  
 Sonnerup, B. U. Ö., & Priest, E. R. 1975, *J. Plasma Phys.*, 14, 283  
 Watson, P. G., & Craig, I. J. D. 1997, *Phys. Plasmas*, 4, 110  
 Watson, P. G., Priest, E. R., & Craig, I. J. D. 1998, *Geophys. Astrophys. Fluid Dyn.*, 88, 165  
 Zweibel, E. G. 1998, *Phys. Plasmas*, 5, 247